Autonomous Robotic Sensing Experiments at San Joaquin River

Amarjeet Singh*, Maxim A. Batalin*, Victor Chen*, Michael Stealey*, Brett Jordan†, Jason C Fisher‡, Thomas C. Harmon‡, Mark H Hansen§ and William J Kaiser*
*Department of Electrical Engineering, University of California, Los Angeles.
‡School of Engineering, Univerity of California, Merced
†Department of Mechanical Engineering, University of California, Los Angeles
§Department of Statistics, University of California, Los Angeles
Email: amarjeet@ee.ucla.edu

***Abstract*— Distributed, high-density spatiotemporal observations are proposed for answering many river-related questions, including those pertaining to hydraulics and multi-dimensional river modeling, geomorphology, sediment transport and riparian habitat restoration. We present here a case study of an autonomous, high-resolution robotic spatial mapping of cross-sectional velocity and salt concentration in a river basin. Several experiments for analyzing the spatial and temporal trends at multiple cross-sections of the *San Joaquin River* were performed during the campaign from August 21-25, 2006. Preliminary analysis from these experiments illustrating the range of investigations is presented. Lessons learned during the campaign are discussed to provide useful insights for similar robotic investigations in aquatic environments.**

I. INTRODUCTION

River observations are important from the perspectives of navigation, water supply, flood control, water quality monitoring and management. Water resource management in arid and semi-arid regions such as the Western U.S. can be extremely challenging in times of drought or flooding. Water managers in some of these regions rely on quantitative water distribution algorithms to balance the needs of municipalities, farms, flood control and aquatic ecosystems. Deterministic river flow and transport models can play a role in determining optimal distributions. Though, for regulatory work, these are often simplified (one-dimensional) routing models that assume complete mixing of chemical species throughout the river cross-section [1]. These routing models can be calibrated using time series data from a network of river gauging stations which record gross flow and, in some cases, temperature and bulk salinity in terms of the water's electrical conductivity (EC) [1].

In heavily managed river basins, such as that of *San Joaquin River* in Central California, a robust network of 14 river gauging stations with a spatial granularity of tens of kilometers is operated and maintained by government agencies. This network provides access to the current gross river conditions via the Internet [2], allowing engineers, scientists, and water resource managers to consider real-time adaptive management of these large and complex systems [3]. In spite of impressive progress towards the automated management of the *San Joaquin River* basin, water resources, population influxes, land use changes and climate change impacts [4] create a demand for the distributed observation of flow and water quality parameters.

Distributed, high-density spatiotemporal observations would be useful in answering many river-related questions, including those pertaining to hydraulics and multi-dimensional river modeling [5], geomorphology, sediment transport and riparian habitat restoration [6]. Such observations would enable distributed model parameterization and enable more detailed water quality forecasting than has been possible in the past. This will also provide policy-makers with the information enabling them to make more informed decisions about issues extending beyond water supply and flood control to the restoration of river habitat and aesthetics However, beyond those for flow field characterization, there are no devices and methods for efficient, high granularity and autonomous measurements of coupled hydraulic and water quality parameters in stream cross-sections.

Infrastructure supported Networked Info Mechanical System (NIMS) was introduced in [7]. A Rapidly Deployable (RD) version NIMS-RD is developed to fill the void for efficient and high granularity two dimensional mapping. In this paper we provide a case study of a campaign at the *San Joaquin River* for mapping the river cross-sectional velocity and salinity, executed from August 21-25, 2006 with NIMS-RD. We performed autonomous robotic sensing experiments at the multiple cross-sections and collected physical samples for detailed lab analysis. Real time data collection facilitated high temporal resolution data. Autonomous motion of the mobile system facilitated high spatial resolution data. The high resolution data was then used for preliminary analysis to learn the spatial distribution. This was followed by several adaptive experiments based on learned phenomena distribution.

In the next section, we discuss the related work done in aquatic sensing. In Section 3, we describe NIMS-RD and briefly go through the installation procedure for the system. Section 4 provides a discussion on the experimental design followed by results and discussion based on those experiments in Section 5. Section 6 mentions several important lessons learned during this campaign that also guide the future work discussed in Section 7.

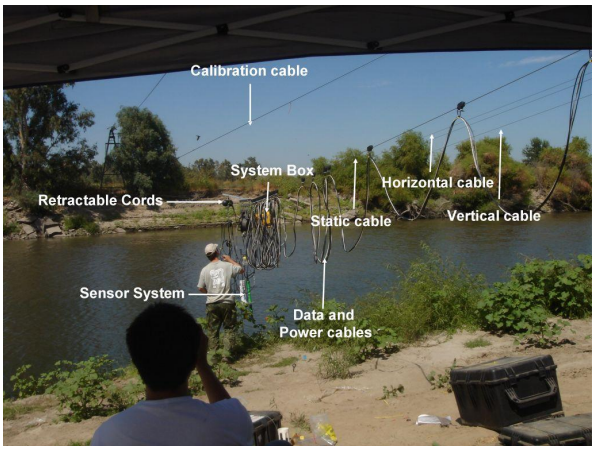

Fig. 1: Rapidly Deployable NIMS system used at San Joaquin

II. Related Work

Several prototype sensing systems have been used for sensing the aquatic systems at different scales. Buoyed or moored deployment platforms exist which can provide vertical profiling capabilities over long time periods at key locations [8], [9]. Networked Aquatic Microbial Observing System (NAMOS) [10] employs a system of static Buoys with a fluorometer (a device for measuring fluorescence, a measure of chlorophyll) and an array of 6 thermistors, each at different depth and a boat equipped with fluorometer and thermistor to provide water surface measurements. The system in its current form has limited capabilities in terms of providing cross-sectional phenomena distribution.

Autonomous underwater vehicles (AUVs) have been used extensively by the oceanographic community, and more recently in lakes and large rivers [11]. However, greater currents and confined operating space associated with small to moderately sized rivers limit the applicability of AUVs in these systems.

The Rivernet Monitoring Program is an effort towards providing high resolution (temporal) measurement of nitrate using in-stream nutrient analyzers [12]. However the instrumentation measures a single point within the flow stream and hence only provides temporally high resolution data, without any spatial resolution. There has been comparatively less progress in regard to high resolution autonomous two-dimensional sampling of rivers. Researchers commonly survey stream velocity by manual operations, for example suspending sensors from bridges [13]. Literature survey reveals that this is for the first time that such an extensive set of experiments have been performed using an autonomous robotic system, performing high resolution spatial mapping of cross-sectional velocity and salt concentration in a river basin.

III. NIMS-RD: Infrastructure supported autonomous robotic system

Rapidly Deployable Networked InfoMechanical System (NIMS-RD), used at San Joaquin is shown in Fig. 1. The corresponding schematic version for better understanding is shown in Fig. 2. Static cable is used to support the complete infrastructure. To anchor the static cable, natural/man-made

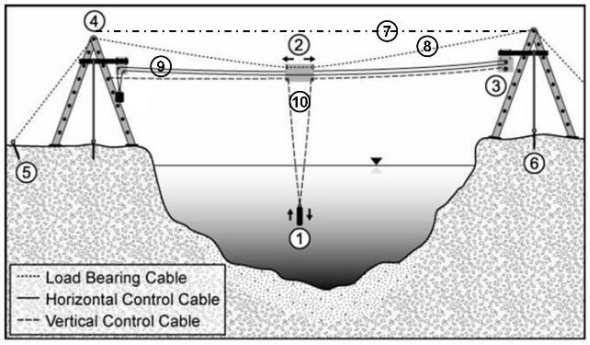

Fig. 2: NIMSRD System is shown in a schematic view: 1: Sensor System, 2: System Box, 3: Motor Controller, 4: Supporting Towers, 5 and 6: Anchor systems, 7: Calibration Cable, 8: Static Cable, 9: Horizontal Cable, 10: Vertical Cable

infrastructure was used in place of the supporting towers. Winches were used to increase the tension on the static cable to avoid excessive cable deflection due to the system weight (that could potentially disturb the localization calibration of the system). The cable is able to support a maximum tension of 3700 pounds while the maximum tension on our system was close to 750 pounds which was well within the safety limits.

The horizontal and the vertical cable are connected on the near shore side to the motor controller. The controller has two motor systems controlling the horizontal and vertical motion of the system respectively. It was ensured that both of these cables have sufficient tension to provide secure actuation without slipping. Both of these motors are controlled simultaneously using a serial interface. This results in a smooth and accurate motion of the system in the two dimensions. Retractable cords were used with the vertical festooning (comprising of the data and the power cables) connected to the sensor system to avoid entangling of these cables during the vertical descent of the node under the water surface.

Index markings on the calibration cable were used to calibrate the sag in the system and provide accurate localization. Post calibration, the system localization was found to be accurate within 2 cm over long duration operations. River monitoring sampling requirements demand that estimating the salt concentration at different depths, from the surface to the bottom is important. Sensing at the lowest point close to the river floor without damaging the sensor system was made possible through accurate sounding. Sounding is the process used for physically determining the bathymetry of the river cross-section.

Power was delivered to the sensor system using a multi conductor cable. Serial interfaces from the sensor system were supported using a serial to ethernet bridge interface, supported by an embedded control and sampling system. Power supply, power control, sensor interface and long range communication were all integrated into a sensor node supported with the sensors and by the NIMS system. Real time data monitoring was performed at the near shore side to ensure that data from each sensor is collected without any error.

The following sensors were used at different stages of

(a) Transect1

(b) Transect2

Fig. 3: Pictures taken for the two transects selected for sensing

the campaign for monitoring different phenomena:

1) Hach Environmental's Hydrolab Minisonde 4a [14]: Sensing temperature, pH and specific conductivity. Sensing rate is 0.1 Hz in internal logging mode and 1 Hz when sending the data over the serial port. It can not simultaneously log internally and send the data over the serial port. It works with external power and/or battery (AA) power.
2) Hach Environmental's Hydrolab DS5 [14]: Sensing depth, oxidation reduction potential, turbidity and Luminescent Dissolved Oxygen (LDO). Sensing rate is 0.1 Hz in internal logging mode and 1 Hz when sending the data over the serial port. It can simultaneously log the data internally and send it over the serial port at their respective rates. It works with external power and/or battery (C) power.
3) Satlantic's ISUS sensor [15]: Sensing nitrate concentration. Sensing rate is approximately 1 Hz both for internal logging and for sending the data over the serial connection. It only sends the data over the serial connection and has no memory for internal logging. It only works with external power.
4) Sontek's Argonaut-ADV [16]: Used for flow monitoring. Sensing rate is 0.1 Hz both for internal logging and sending the data over the serial connection. It can simultaneously log the data internally and send it over the serial port. It only works with external power.
5) Physical sampling device: The device uses dual spring loaded syringes to collect water samples. It collects approximately 70 to 80mL of water, in two syringes, at a time. It uses a system that triggers the action of a spring-loaded device controlled by a solenoid actuated by the sensor node power system.

Fig. 4 shows the picture of all the four sensors and the physical sampling device.

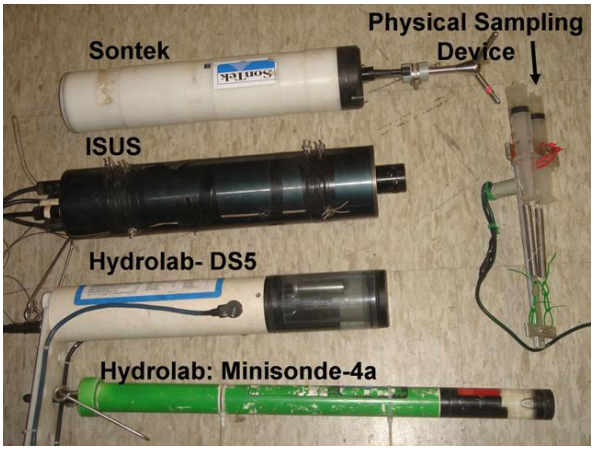

Fig. 4: Complete set of sensors along with physical sampling device used during the campaign

IV. Experimental Design

The scientific objective of this investigation was to characterize the transport and mixing phenomena at the confluence of two distinctly different rivers: the Merced River (relatively low salinity) and the agricultural drainage-impacted San Joaquin River (relatively high salinity). High spatial resolution sensing experiments were performed at two different transects. The first transect was selected at the specific location for the following reasons:

- Leveraging the two obsolete steel towers associated with the past historical stream gauging methods for anchoring the system and to use the cable between those towers for supporting the system cables overnight at a suitable elevation above the river surface.
- This transect was further downstream from the confluence point of *San Joaquin River* and Merced River (approximately 290 meters downstream) and was representative of the conditions within the downstream portion of the confluence mixing zone.

The second transect was selected upstream as it was very close to the confluence of the two rivers (approximately

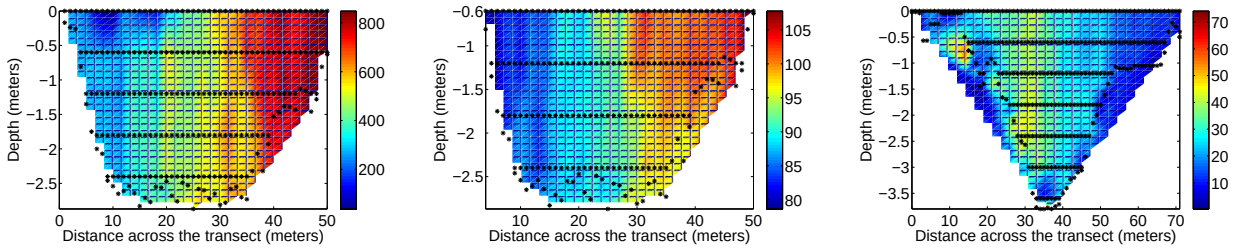

(a) Specific conductivity at the first transect during raster scan on August 23 morning

(b) Nitrate at the first transect during raster scan on August 23 evening

(c) Flow distribution at the second transect during raster scan on August 25 morning

Fig. 5: High granularity (raster) scans at the two transects for different parameters

130 meters from the confluence point) and hence was representative of the conditions in the upstream portion of the confluence mixing zone.

Fig. 3a and 3b show the pictures taken for the two transects respectively. The first transect was 50 meters wide while the second was 70 meters wide.

The basic experiment performed at both transects was to sense at uniform density (i.e a raster scan) along the cross-section of the river. Sampling density for the scan was selected to be 1 meter across the river and 0.6 meters along the depth.

Dwelling time at each sensing location was fixed to 30 seconds to comply with the requirements associated with both the settling time of sensor systems and the requirement to collect multiple samples at each location to verify sampling stability. Fixing the dwelling time also ensured uniformity across several raster scans at both the transects.

Since we are addressing a spatially distributed phenomena, a common approach in statistics is to use a rich class of probabilistic models called Gaussian Processes (GPs) [17]. Using such models, one can quantify the informativeness of a particular location, in terms of the uncertainty about our prediction of the phenomena, given the measurements made by the mobile robots. To quantify this uncertainty, we use the mutual information (MI) criterion [18]. If the phenomenon is discretized into finitely many sensing locations $\mathcal{V}$, then for a set of locations $\mathcal{P}$, visited by the mobile robot, the MI criterion is defined as:

$$\mathrm{MI}(\mathcal{P}) \equiv H(\mathcal{X}_{\mathcal{V}\setminus\mathcal{P}}) - H(\mathcal{X}_{\mathcal{V}\setminus\mathcal{P}} \mid \mathcal{X}_{\mathcal{P}}), \qquad (1)$$

where $H(\mathcal{X}_{\mathcal{V}\setminus\mathcal{P}})$ is the entropy of the unobserved locations, and $H(\mathcal{X}_{\mathcal{V}\setminus\mathcal{P}} \mid \mathcal{X}_{\mathcal{P}})$ is the conditional entropy after observing sensing locations $\mathcal{P}$. Hence mutual information measures the reduction in uncertainty at the unobserved locations. In particular, we learned a non-stationary Gaussian Process model by maximizing the marginal likelihood [17] using the specific conductivity data for half (125 locations out of the total of 250) of the observation locations from the raster scan. We then used the mutual information criterion to greedily select a set of 30 and 50 locations each, from the remaining 125 locations and evaluated this GP model based adaptive sampling approach. Any such adaptive approach, based on learned distribution, will provide a subset of locations to sample. Using the data from this subset and the learned model, the phenomena distribution can then be predicted at the unobserved locations. This will save considerable sampling time, otherwise spent in dense raster scan sampling.

Measurement of phenomena characteristics not accessible to in situ sensing (for example determining the concentration of contaminants for which the sensors are not available) requires laboratory analysis of physical samples from the river. This requires samples to be taken at different depths to analyze at a later stage. Fig. 4 shows a picture of the physical sampling device that was developed to facilitate the collection of samples in the field from any desired location. A sample quantity of approximately 30 ml is sufficient for the laboratory analysis of most phenomena of interest in this application area.

Logging the data in real time using the serial port connectors on the sensors provides several advantages. As discussed earlier, it increases the logging rate for both Hydrolab Minisonde-4a and Hydrolab DS5. Additionally logging in real time ensures robustness against the system failure which could simply be detected based on graphical visualization. We monitored the data in real time and this helped at several occasions when we were able to detect that the data cable was disconnected from the sensor.

V. Results and Discussion

The first day of the campaign was spent setting up the system and addressing all the problems that arise under difficult environmental conditions. The next four days were spent performing several experiments at the two different transects. Piecewise bilinear interpolation is performed between the sampling locations to create the surface distributions. For each surface distribution, the mean at each location is considered as the sampled value at that location.

A. Spatial Trends

Spatial distribution of three of the several measured parameters sampled with high granularity raster scans in the stream cross-sections is shown in Fig. 5. The dots in the figure represent the sampling locations. Based on sampling density discussed earlier, a total of 250 locations were sampled at the first transect while a total of 292 locations were sampled at the second transect. The duration of each raster scan at the first transect was approximately 2 hours and 40 minutes while the total time duration for raster scan at the second transect was approximately 3 hours and 5 minutes. The first transect was approximately 290 meters

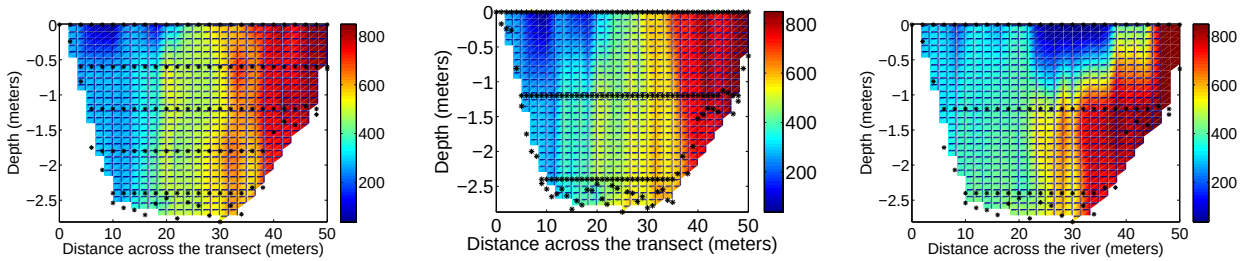

(a) Sparse sampling across the transect (b) Sparse sampling along the depth (c) sparse sampling using the NIMS system

Fig. 7: Effect of sparse sampling on specific conductivity at the first transect

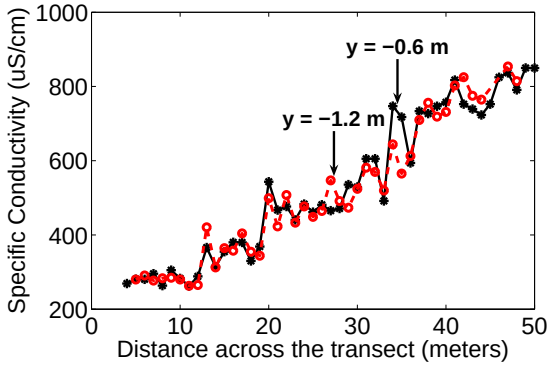

Fig. 6: Spatial variation of specific conductivity at two different depths during the raster scan in the morning of August 23.

downstream from the confluence point while the second one was approximately 130 meters downstream from the confluence point. As per the coordinate system, the water stream on the near side (lower x coordinate value) is coming from the Merced River while the water stream on the far side is coming from the *San Joaquin River* .

Fig. 5a shows the distribution of specific conductivity ($\mu S/cm$) as measured by Minisonde-4a at the first transect during a raster scan performed in the morning of August 23. Fig. 6 represents the spatial distribution at two different depths of 0.6 meters and 1.2 meters for the corresponding raster scan. Fig. 5b shows the distribution of nitrate concentration ($\mu Mol/L$) as measured by the ISUS nitrate sensor along the same cross-section during the evening of August 23. Due to the difference in the lengths of ISUS and Minisonde-4a, ISUS sensor was above the river surface for all the observations taken at $y = 0$. Therefore, only the readings for depths less than 0 are considered for creating the surface distribution.

Strong vertical correlation can be easily observed in the comparison of spatial variation curves at different depths, shown in Fig. 6. Additionally, from the two surface distributions it can be clearly observed that there exists a vertical profile with three different zones. Two zones on either end representing individual streams from *San Joaquin River* and Merced River while the middle one representing the confluence mixing zone.

Fig. 5c shows the flow distribution (cm/s) as measured by Argonaut-ADV along the cross-section of the second transect on the morning of August 25. As expected, there is near zero flow close to each bank and close to the river floor, while there is a uniform flow in the middle of the river.

B. Adaptive Sampling

Fig. 7 shows the distribution of specific conductivity when a sparse sampling density is considered at the first transect. Fig. 7a and 7b are the interpolated surfaces when only a subset of locations from dense raster scan, performed on morning of August 23 are considered. Fig. 7c represents the surface distribution using the data values from an actual sparse scan performed by the NIMS node on August 24. Points in the figure represent the locations considered for creating the phenomenon surface.

Fig. 7a represents the distribution of specific conductivity when sparse density is considered along the cross-section, keeping the density along the depth same. The total time, including the sampling and travel time, required for such a scan will be approximately 1 hour and 35 minutes. Fig. 7b represents the distribution of specific conductivity when sparse density is considered along the depth keeping the density along the cross-section same. The total time required for such a scan will be approximately 1 hour and 40 minutes. These surface plots visually appear similar to those created using all the sampled locations. This can be taken as a preliminary indication that the phenomena shows a smooth distribution with no abrupt peaks. Hence it may not require very dense sampling. Moreover, this distribution, if learned, can be utilized to sample adaptively. With the aid of learned distribution, sampling at only a few locations could provide the complete phenomena distribution. We plan to perform detailed analysis of the collected data in the future to identify models that could help us sample adaptively.

Fig. 7c is the surface distribution created by a sparse sampling of 85 locations with dwelling time at each location reduced to 15 seconds. This scan was performed on August 24 around the same time as the dense scan demonstrated in Fig. 5a. The total time, including the sampling and travel time, for this scan was approximately 36 minutes. As can be easily seen, the interpolated surface is different from the surface distribution for August 23. This difference can be attributed to two reasons. Firstly, the phenomena shows temporal variation as can be seen from Fig. 9. Secondly, there is considerable short term temporal variation as is observed in Fig. 9c. Dwelling for 15 seconds in the

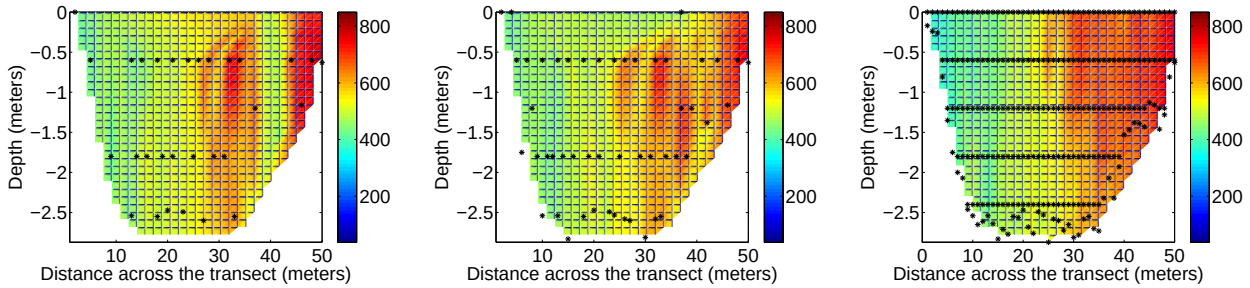

(a) Greedy selection of 30 locations (b) Greedy selection of 50 locations (c) Raster scan

Fig. 8: Predicted distribution of specific conductivity at the cross-section of the first transect using Gaussian Process based modeling and comparison with the distribution sampled by raster scan around the same time, the previous day

confluence zone, where water from the two rivers is mixing, may not provide stable uniform observations.

As a preliminary testing of an adaptive approach, we trained a Gaussian Process using a subset of locations from the raster scan performed on August 23. Next NIMS-RD performed sampling at the selected subset of locations. Consequently the phenomena is reconstructed by predicting the values at the unobserved locations using the learned model and observed values. Finally the complete set of values, predicted and sampled, are interpolated to generate the surface distribution. Fig. 8 shows the distribution of specific conductivity at the cross-section of the first transect with the surface being interpolated using the values predicted from a small subset of observed values and learned model. Fig. 8a shows the predicted surface when only 30 out of 250 locations, selected greedily based on Mutual Information, are sampled. Fig. 8b shows the predicted surface when only 50 out of 250 locations, selected greedily based on MI, are sampled. The points in each plot represent the set of locations selected by the algorithm. Total time duration for sampling 30 locations was almost 20 minutes while for 50 locations it was around 31 minutes. This is considerably smaller sampling time, compared with 2 hours and 40 minutes for the complete raster scan. Thus, learning a model for phenomena distribution and accordingly performing an adaptive sensing could save a lot of sampling time.

Fig. 8c represents the distribution of specific conductivity as was sampled using the raster scan, at the same time during the previous day. If the distribution of specific conductivity is assumed to be the same during the same time on two consecutive days, then this distribution can be considered as a ground truth for analyzing the prediction quality of the Gaussian Process based sampling approach. The predicted surface using the Gaussian Process based approach appears visually similar to the actual phenomenon distribution. Still, there is considerable difference between the predicted surface and the ground truth. This could be attributed to several reasons. The primary reason based on our analysis is the temporal variation in the phenomena distribution. The model was learned based on a raster scan performed at the previous day during a different time of the day. The model in its current form, does not take into account the temporal variations in the phenomena distribution. This may lead to inaccuracy in predicting the subset of locations to sample and in predicting the phenomena at unvisited locations. Temporal variations in the phenomena distribution are discussed in the next section. Part of the non smooth surface distribution can also be attributed to the bilinear interpolation used for creating these surfaces. These are only the preliminary results from one of the several adaptive sampling approaches we intend to study for modeling the distribution of several phenomena.

C. Temporal Trends

To analyze the short term temporal trends of the phenomena distribution, we selected a set of 7 locations at a depth 1.2 meters below the water surface. At each location we increased the dwell time to 5 minutes. To analyze the long term temporal trends, we observed the distribution of specific conductivity at a depth of 1.2 meters across raster scans performed over two consecutive days. Fig. 9 shows temporal variation of specific conductivity as observed during several experiments. The x axis represents the location along the cross-section of the river stream.

Fig. 9a shows the distribution of specific conductivity at a depth of 1.2 meters across raster scans performed on August 23 and August 24 at the first transect. As can be observed, there is considerable difference not just across different times during the day but also across same time for consecutive days.

Fig. 9b shows the mean value during the dwelling time of 5 minutes at different locations along the cross-section of river. Fig. 9c shows the time series measured at a distance of 15, 30 and 40 meters along the cross-section of the river. As is clear from the plots, there is considerable temporal variation even in a short duration of 5 minutes, especially towards the far side of the river. It can be observed that the time series for each spatial point has different characteristics (much more extreme excursions in the middle than at the edges). This further necessitates longer dwelling time in the middle confluence zone as compared to the two ends. The results of these experiments are expected to permit the development of optimized sampling methods.

D. Physical Sampling

The physical sampling device was used to collect water samples from several locations along the cross-section of the first transect. Several lab tests show detectable

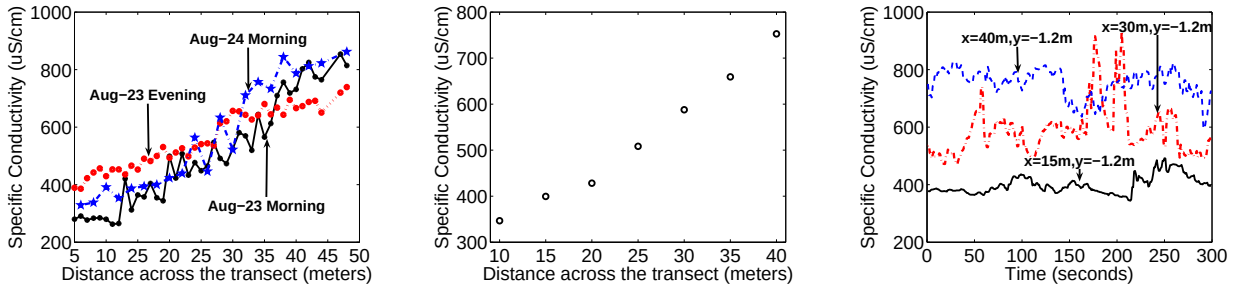

(a) Variations at 1.2 meters depth during different raster scans

(b) Short term mean across the transect

(c) Short term variations at three locations

Fig. 9: Temporal trends for specific conductivity at the first transect

amounts of boron and phosphate, elements interesting to the environmentalist but can not be detected using the currently available suite of sensors. Additionally, we also tested the collected samples for nitrate concentration and the measurements were well in accordance with the measurements taken by ISUS sensor in the river. This can be viewed as both a validation of the calibration of the sensor and precision of the autonomous collection of physical samples from any location in the cross-section of the river.

VI. Lessons Learned

The application of autonomous robotic sensing in complex river system environments presents a wide range of challenges that are not encountered in a typical laboratory systems. While this NIMS system and the campaign described here has provided data of immediate value to the urgent environmental investigations, it has also provided lessons that guide further advances in the NIMS system implementation.

First, the installation of the system infrastructure represents a time investment that must be minimized in order to expedite the deployment and permit rapid river characterization. By decreasing the deployment time, more transects may be characterized with a single system in the available investigation time (itself limited by the time period over which the phenomena may lie in a range of interest). Deployment experience has shown that detailed inspection and preparation of a deployment site reduces the logistics burden associated with the equipment transport and may also permit the convenient use of vehicles for transport. Prior site inspection and preparation also permits the advance installation of anchoring systems and identification of pathways for convenient access by personnel. It is also important to note that in this application, due to the river flooding, our deployment sites were inundated by flood waters merely a few months prior to this deployment. Thus, rapid planning and adaptation are required, in general, for successful monitoring campaigns.

The use of cable infrastructure supported mobile system introduces high precision in transport. However, to exploit this capability, deployment design limits must be incorporated. First, the essential horizontal and the vertical drive cables enabling the corresponding motion of the sensing node, require an appropriate tension. A low tension on either of these cables would cause non-deterministic cable motion due to a slipping action encountered at the cable actuators. High tension at the cable results in extra load on the motor system for rotating the corresponding pulley actuators. This results in excessive motor actuator heating and ultimately a need to disable these devices during operation for protection. To avoid this problem, the NIMS design incorporates elastic spring tensioner. This facilitates required tension while permitting a horizontal compliance and easing the required precision in the cable length selection for tension adjustment. During this campaign, as in others, each installation provides further guidance for the adjustment and site selection associated with the deployments. These findings are then incorporated into the system documentation for time efficient future deployments.

Another problem associated with the use of public environment is to make sure that the campaign does not disturb the routine work of individuals using the same environment. In our case, some of the fishermen used to go around in the boats in the river later in the day. This would have required us to take down the cable infrastructure every evening and reinstall it the next morning, resulting in valuable campaign time being wasted. We worked around the problem by supporting our cable infrastructure with the cable running between the the two steel towers associated with the past historical stream gauging methods at the first transect, making sure it is at a height where anyone in a small boat could pass from underneath. No such option was available at the second transect so we let the cables sink to the river bottom every night, without taking them out completely from the far side of the river. In the morning, it was then easier to restore the infrastructure without significant delays.

Nature brings with it the severe conditions that cause degradation to equipment resulting in in-field failure. This is critical to avoid, since the value of acquired data is high and critical to the end users. Several challenges have been addressed in this field and have resulted from detailed findings from multiple deployments. First, electronic components and infrastructure components must be protected from moisture and be also equipped to withstand indefinite immersion in potentially corrosive water solutions. Further sources of failure are associated with the integrity of data transmission cables and connectors. An essential step is the introduction of redundancy in the data capture. This was accomplished by applying both real time monitoring (relying on data transmission cables) as well as the simultaneous

archiving of data in the sensor systems themselves using the nonvolatile memory storage. Thus, in the event of data transmission errors or failures, data still remains available. Finally, reliability of sensor node power systems presents yet another concern. In particular, data acquisition campaigns may be suddenly extended to accommodate new findings and requirements. Thus, in addition to local energy storage in primary batteries, power is also supplied to sensors to provide a long-term, reliable power source for indefinite operation. All of these design features proved to be essential for the success of the campaign described here.

VII. Conclusions and Future Work

In this paper we describe a case study for an autonomous, high resolution robotic aquatic sensing and its deployment in an important river system. Experimental investigations were directed to resolving some of the most important phenomena. Prior results have shown that the required sampling accuracy will rely on effective adaptive sampling techniques that not only provide high fidelity sampling, but also high sampling speed in dynamically variable environments. Several experiments varying from uniform sampling for estimating spatial trends to adaptive sampling experiments and experiments for estimating the temporal trends were performed during the campaign at the *San Joaquin River* . Datasets collected during the campaign are proving useful in providing a means for characterizing mixing at river confluences, hydraulics, geomorphology, total salt load estimates and detection of other contaminants. Physical water samples were collected using the autonomous robotic system, from several locations and depths in the river providing a measure of contaminant concentration for those components not detectable by the available sensor suite. Important lessons learned during the campaign provide a rich set of insights into the preparation for any such campaign for aquatic monitoring and for guiding further advances in autonomous robotic sensing systems.

In addition to the development of additional robotic sensing systems, the results of this campaign will also lead to the development and verification of adaptive sampling methods that are optimized for river system monitoring. This will include the development of increasingly autonomous calibration and sounding procedures. Future deployments of the NIMS system will also explore flow and contaminant transport phenomena throughout the complete river confluence and at its tributaries.

Acknowledgment

This material is based upon work supported in part by the US National Science Foundation (NSF) under Grants ANI-00331481. Any opinions, findings, and conclusions or recommendations expressed in this material are those of the authors and do not necessarily reflect the views of the NSF. The authors also acknowledge the support of Henry Pai, Yeung Lam, Jon Binney, Andre Encarnacao and Ignacio Zendejas for the system development and deployment during the campaign.

References

[1] "Calsim ii simulation of historical swp-cvp operations," *California Department of Water Resources Technical Memorandum Report*, '2003.

[2] (2006) California data exchange center. [Online]. Available: http://cdec.water.ca.gov/

[3] N. Quinn, K. Jacobs, C. Chen, and S. W.T., "Elements of a decision support system for real-time management of dissolved oxygen in the san joaquin river deep water ship channel," *Environmental Modelling and Software*, vol. 20, pp. 1495–1504, 2005.

[4] L. D. Brekke, N. L. Miller, K. E. Bashford, N. W. Quinn, and J. A. Dracup, "Climate change impacts uncertainty for water resources in the san joaquin river basin, california," *Journal of the American water resource association*, vol. 40, pp. 149–164, February 2004.

[5] R. Hardy, P. Bates, and M. Anderson, "The importance of spatial resolution in hydraulic models for floodplain environments," *Journal of Hydrology*, vol. 216, pp. 124–136, March 1999.

[6] J. Wheaton, G. Pasternack, and J. Merz, "Spawning habitat rehabilitation i. conceptual approach and methods," *Intl. Journal River Basis Management*, vol. 2, pp. 3–20, 2004.

[7] R. Pon, M. Batalin, J. Gordon, M. Rahimi, W. Kaiser, G. Sukhatme, M. Srivastava, and D. Estrin, "Networked infomechanical systems: A mobile wireless sensor network platform," in *IPSN'05*, pp. 376–381.

[8] J. V. Reynolds-Fleming, J. G. Fleming, and J. Richard A. Luettich, "Portable autonomous vertical profiler for estuarine applications," *Estuaries*, vol. 25, pp. 142–147, 2004.

[9] K. W. Doherty, D. E. Frye, S. P. Liberatore, and J. M. Toole, "A moored profiling instrument," *Journal of Atmospheric and Oceanic Technology*, vol. 16, pp. 1816–1829, 1998.

[10] A. Dhariwal, B. Zhang, B. Stauffer, C. Oberg, G. S. Sukhatme, D. A. Caron, and A. A. Requicha, "Networked aquatic microbial observing system," in *IEEE ICRA*, 2006.

[11] D. R. Blidberg, "The development of autonomous underwater vehicles (auvs); a brief summary,," in *IEEE ICRA*, 2001.

[12] B. P. Usry, "Nitrogen loading in the neuse river basin, north carolina: The rivernet monitoring program," Master's thesis, North Carolina State University, 2006.

[13] B. De Serres, A. Roy, P. Biron, and J. Best, "Three-dimensional structure of flow at a confluence of river channels with discordant beds," *Geomorphology*, vol. 26, pp. 316–335, 1999.

[14] [Online]. Available: http://www.hachenvironmental.com

[15] [Online]. Available: http://www.satlantic.com

[16] [Online]. Available: http://www.sontek.com

[17] M. Seeger, "Gaussian processes for machine learning," *Int. Jour. of Neural Systems*, vol. 14, no. 2, pp. 69–106, 2004.

[18] C. Guestrin, A. Krause, and A. P. Singh, "Near-optimal sensor placements in gaussian processes," in *ICML*, 2005, pp. 265–272.